AIAA 80-0773R

# Analytical and Experimental Results for Bonded Single Lap Joints with Preformed Adherends

James Wayne Sawyer* and Paul A. Cooper†
*NASA Langley Research Center, Hampton, Va.*

**A theoretical and experimental study is conducted to investigate the load transfer of a single lap joint in which the adherends are preformed so that the angle between the line of action of the applied in-plane force and the bond line is reduced. The preforming of the adherend reduces the moment resultant in the adherend at the edge of the overlap region, which reduces both the maximum peel and shear stresses in the adhesive and gives a more uniform shear distribution in the adhesive. An increase in static load transfer of up to 120% is shown, and several orders-of-magnitude increase in fatigue life are achieved with modest preform angles. Thus, sizable benefits can be obtained in the fatigue life or additional load capacity of bonded single lap joints by preforming the adherends.**

## Nomenclature

$a$ = length between edge of bond and bend (see Fig. 1)
$A$ = extensional stiffness of adherend
$c$ = one-half the overlap length (see Fig. 1)
$D$ = plate stiffness of adherend (see Appendix)
$E$ = adherend Young's modulus
$E_a$ = adhesive Young's modulus
$G_a$ = adhesive shear modulus
$\ell$ = length of adherend from point-of-load application to beginning of overlap
$P$ = adherend load resultant, force per unit width
$t$ = adherend thickness
$w_i$ = lateral displacement of adherend in section $i$
$x$ = lineal measurements defined where used
$\eta$ = adhesive thickness
$\theta$ = preform angle (see Fig. 1)
$\nu$ = Poisson's ratio of adherend material
$\sigma$ = applied normal stress in adherend
$\sigma_y$ = adhesive normal stress in $y$ direction
$\sigma_x$ = adhesive normal stress in $x$ direction
$\tau$ = adhesive shear stress
$\tau_{av}$ = nominal shear stress in bond line, $P/2c$
$\phi$ = angular measure between line of action of applied force and plane of bond (see Fig. A1)

## Introduction

DUE to the stress concentrations in adhesively bonded single lap joints, an increase in bonding area does not increase proportionally the amount of load which can be safely transferred. In fact, at some point, a further increase in bonding area will give no additional load-transfer capability. Mylonas[1] and Das Gupta and Sharma[2] suggest that a geometric modification consisting of preforming the adherends of a single lap joint could reduce the stress concentrations. This reduction is caused by decreasing the angle between the line of action of the applied in-plane force and the bond line (see Fig. 1), thereby reducing both applied bending moments and transverse shear forces much the same as in a scarf joint. Preforming the adherends of single lap joints has not been thoroughly investigated.

Presented as Paper 80-0773 at the AIAA/ASME/ASCE/AHS 21st Structures, Structural Dynamics and Materials Conference, Seattle, Wash., May 12-14, 1980; submitted June 11, 1980; revision received Jan. 30, 1981. This paper is declared a work of the U. S. Government and therefore is in the public domain.

*Aerospace Engineer, Structures and Dynamics Division.
†Aerospace Engineer, Structures and Dynamics Division. Associate Fellow AIAA.

Results are presented from an analytical and experimental investigation to determine the effect that preforming the adherend has on the stress distributions and strengths of bonded single lap joints. The analytical investigation used a closed-form analysis similar to that of the classical analysis of Goland and Reissner[3] and a two-dimensional quasi-nonlinear finite-element analysis similar to that of Ref. 4 to study in detail the stress distributions in the ASTM D 1002-72 specimen[5] with a 1.27-cm (0.50-in.) overlap and preformed adherends. The finite element analysis is used to check the accuracy of the closed-form analysis. A parametric study is conducted using the closed-form analysis to determine the optimum adherend preform angle for typical adherend and adhesive material properties and joint geometries. The experimental investigation includes numerous tension-to-failure tests to determine the effect that preforming the adherends has on the ultimate static strength of typical bonded joints. A photoelastic test is also conducted to show the changes in the stress distribution in the joint due to preforming the adherends.

Due to the high stress concentrations near the edge of the overlap region in the adhesive, joints are usually designed for fatigue rather than static strength. In fact, design-allowable stresses for single lap joints are generally taken to be 30% of the static ultimate strength because of fatigue. The reductions in stress concentrations obtained by preforming the adherends of single lap joints should significantly improve the fatigue strength. Thus, fatigue tests are also conducted to determine the effect of preforming the adherends on the fatigue strength of typical bonded single lap joints. Because of program and time constraints, only a limited number of low-cycle fatigue tests are performed. Test variables include both preform angle and overlap length.

## Analysis

### Analysis Methods

*Approximate Nonlinear Finite Element Analysis*

The finite-element code, SPAR,[6] is used to analyze the preformed adherend single lap joint. The finite element mesh used in the analysis is shown in Fig. 2. An assumed stress field formulation[6] with a minimum complementary energy method is used in the solution. A fine mesh is used in areas near the ends of the joint where large stress gradients normally occur. A singularity exists in a two-dimensional continuum analysis at the re-entrant corner (see Fig. 2) formed by the adherend-adhesive interface; however, the singularity does not affect the results presented herein. A total of 768 nodes and 640 triangular and quadrilateral membrane elements are used in the analysis. Results from similar analyses for models with a

smaller and larger number of elements indicate that the modeling used is adequate in the regions under inspection.

Results from the analysis of a straight single lap joint described in Ref. 4 show the importance of properly accounting for the bending moment in the joint. This bending moment is due to the eccentricity of the loading and to the deformation of the adherends as the load is applied. The dependence of the moment on the applied load makes the problem geometrically nonlinear. Although the SPAR computer code is linear, an approximation to the nonlinear behavior is obtained using SPAR by first obtaining a linear solution with the bending moment based on the undeformed shape. The initial stress stiffness matrix associated with the applied load and the resulting deformations are calculated and then added to the initial stiffness matrix. Next, the linear SPAR analysis is rerun with the modified stiffness matrix to give a one-step approximation to the nonlinear problem. This process is repeated until convergence of the solution is achieved. This procedure is shown[4] for a single lap joint with straight adherends to give converged results that are in excellent agreement with a nonlinear finite difference solution.

*Modified Classical Analysis*

An analysis technique following the procedures of Goland and Reissner[3] for a single lap joint with a flexible adhesive as modified in Ref. 2 for preformed adherends is presented in the Appendix. The development of the adhesive shear and peel stress equations is similar to that of Ref. 3 but with plate behavior being treated consistently throughout the development; whereas in Ref. 3, beam theory is used for load-displacement equations and boundary conditions, while plate theory is used to develop the moment equilibrium equations. In addition, small terms ignored in Ref. 3 on the order of the product of the adhesive thickness and the adherend thickness $t$, and the adhesive thickness squared are retained for completeness. Also $\tan\phi$ was replaced by $\phi$ and $\cos\phi$ by 1.0 in Ref. 3 but are retained in the current analysis. The stresses are assumed constant through the adhesive thickness, and the adhesive direct stress parallel to the adherends is assumed negligible. The analysis is for adherends and adhesives that are linear elastic materials with mechanical properties as given in Table 1. The shear deformations in the adherends and the influence of the adhesive on the flexural stiffness of the joint are assumed negligible. Results based on these same modifications for a straight adherend single lap joint[4] indicate the validity of these assumptions. The Ref. 4 results also show that the solution is accurate for qualitative evaluation of the influence of parametric variations on the shear and peel stresses along the midplane of the adhesive.

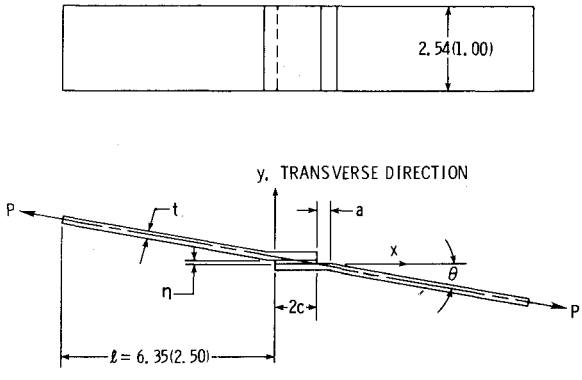


**Fig. 1 Bonded single lap joint with preformed adherends. Dimensions in centimeters (inches).**

**Analytical Results**

*Effect of Preform Angle*

Shear, peel, and in-plane tensile stress distributions through the midplane of the adhesive determined using the finite element analysis are shown in Figs. 3-5, respectively, for a 175 kN/m (1000 lbf/in.) applied tensile load per unit width. Stresses are presented as a function of distance along the bondline for preform angles of 0, 5, 10, and 15 deg for aluminum adherends and an epoxy adhesive. The shear stress is normalized by the average applied shear stress $P/2c$ in the joint, and the peel and in-plane tensile stresses are normalized by the average applied stress $P/t$ in the adherend.

The maximum shear and peel stresses (see Figs. 3 and 4) occur near the free edge of the adhesive. In addition, maximum in-plane tensile stress (see Fig. 5) also occurs near the free edge of the adhesive, but the value is considerably smaller than the maximum value of peel and shear stresses. Because the major load transfer in the single lap joint occurs through shear, the uneven shear distribution is an indication of why straight single lap joints have poor load transfer capability.

A preform angle of 15 deg results in the lowest stress conditions in the joint for those angles considered. Note, however, that the 15 deg preform angle is greater than the angle required to geometrically align the adherends in the unloaded joint. The adherends are aligned geometrically when $\theta = \phi$, which from the equation for $\tan\phi$ in the Appendix gives $\theta = 5.2$ deg for a lap joint with $2c = 1.27$ cm (0.50 in.), $t = 0.162$ cm (0.064 in.), $\eta = 0.010$ cm (0.004 in.), and $a = 0.32$ cm (0.125 in.). As the straight lap is preformed to 15 deg, the shear stress concentration drops from 3.55 for the straight lap joint to 1.05, and the shear stress distribution becomes more uniform over the full joint length. The maximum peel stress ratio for the 15 deg preform angle is reduced from 0.65 for the straight lap joint to 0.10, and the maximum in-plane tensile

**Table 1 Mechanical properties of materials used in analysis**

| | Tensile modulus | | |
|---|---|---|---|
| | GPa | psi, $10^6$ | $\nu$ |
| Adhesive | 3.4 | 0.5 | 0.34 |
| Adherends | | | |
| Aluminum | 73 | 10.6 | 0.33 |
| Titanium | 110 | 16 | 0.33 |
| Steel | 207 | 30 | 0.33 |

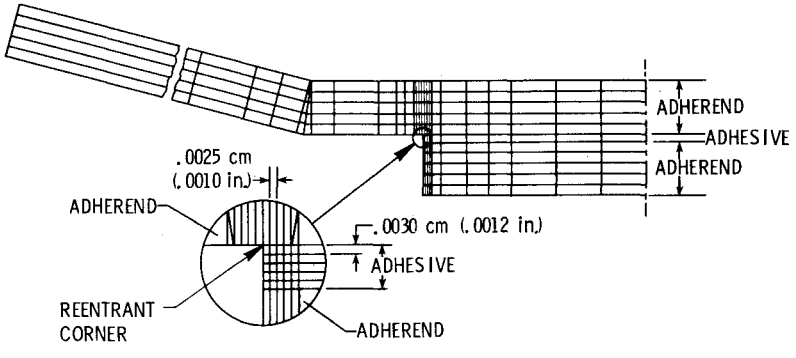


**Fig. 2 Finite element model of preformed single lap joint. Dimensions in centimeters (inches).**

stress ratio from 0.20 for the straight lap joint to 0.04. The large reduction in the maximum stresses and the increased uniformity of the shear stress distribution should result in a large increase in the static load-carrying capability of the joint. Preforming the adherends might be especially effective for adherends fabricated from materials inherently weak in the transverse direction, such as many filamentary composite materials which often fail within the first few plies of the adherend due to transverse normal tensile stress. Stress distributions at other locations through the adhesive are examined using the finite-element analysis, and the results indicate that there is little variation in the stress distributions through the thickness of the adhesive, except near the edge of the lap joint. The results indicate, however, that the variations through the thickness near the edge of the overlap are considerably reduced for large preform angles. Thus, evaluation of the stress distributions through the midplane of the joint is considered adequate to evaluate the influence of preform angle on the stress state in the joint.

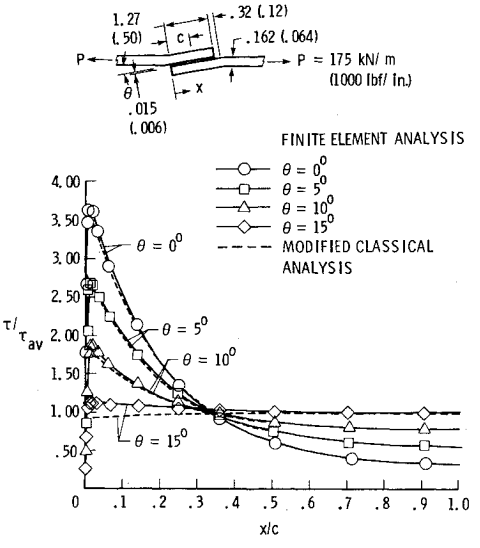


**Fig. 3 Shear stress along the midplane of the adhesive for various preform adherend angles and for aluminum adherends and epoxy adhesive. Dimensions in centimeters (inches).**

*Comparison of Analyses*

To judge the accuracy of the modified classical analysis for the preformed adherends, the adhesive shear and peel stress distributions obtained along the midplane of the adhesive are presented in Figs. 3 and 4 with the stress distributions computed using the nonlinear finite element procedures for various adherend preform angles. The distributions computed by the two methods are considered to be in excellent agreement. Results from the modified analysis predict that the maximum shear stress will occur at the edge of the overlap region because of assumptions made in the development of the analysis procedure, whereas results from the finite element analysis indicate that the maximum will occur slightly away from the edge. However, the predicted maximum values are in close agreement. Thus, the form of the stress distribution and the stress level obtained using the modified classical analysis is considered adequate for qualitative evaluation of the influence of geometry and material properties on the midplane adhesive stresses of single lap joints with preformed adherends.

A well-established failure theory has not been developed for bonded joints. For this investigation, the distortional energy failure criterion commonly associated with Von Mises is selected as a failure criterion to determine the optimum preform angle. The failure stress parameter is given by the equation $J=\sqrt{\sigma_y^2+3\tau^2}$, where $\sigma_y$ is the maximum direct stress acting transverse to the plane of the bond and $\tau$ is the maximum shear stress at the midplane of the adhesive. As the preform angle is varied, the angle which results in the minimum value of the failure stress parameter can be determined for a joint fabricated from the desired materials with a specific overlap length. The stress parameters calculated for five adherend preform angles using the nonlinear finite element analysis and also calculated using the modified analysis are shown in Fig. 6 for an applied load of 175 kN/m (1000 lbf/in.). The results agree well, with the optimum preform angle obtained using the modified classical analysis only slightly higher than that obtained using the finite element analysis.

*Parametric Studies*

The influence of various parameters including applied load, adhesive and adherend material properties, and geometry on the failure stress parameter is shown in Figs. 7-12. If it is assumed that failure will occur for a given value of the stress

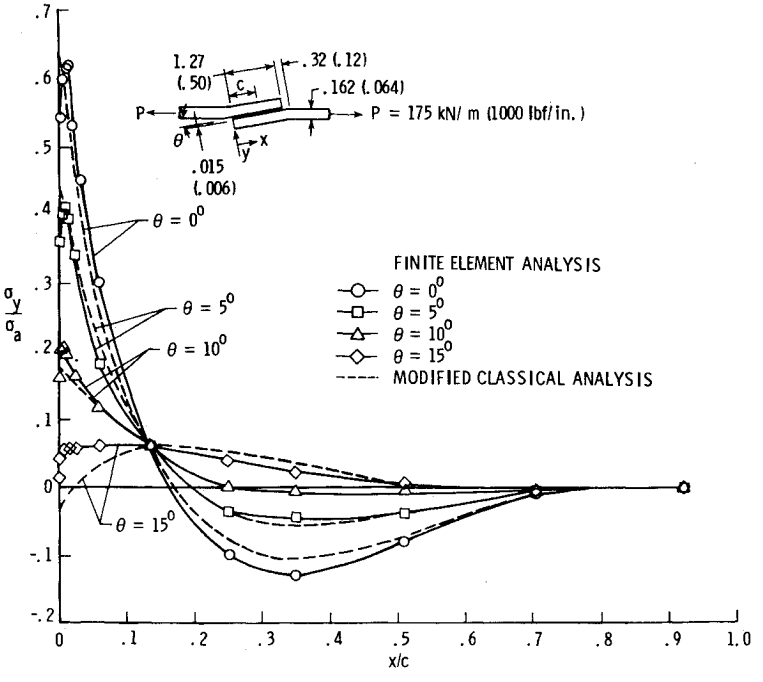


**Fig. 4 Peel stress along the midplane of the adhesive for various preformed adherend angles and for aluminum adherends and epoxy adhesive. Dimensions in centimeters (inches).**

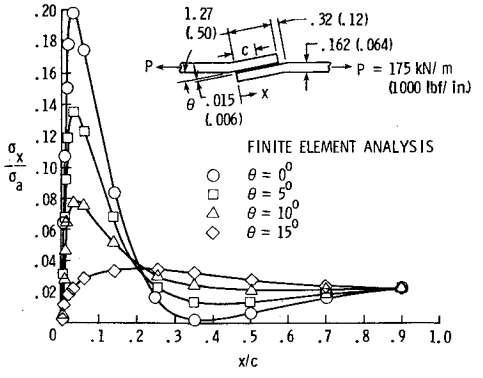


**Fig. 5 In-plane tensile stress from finite element analysis along the midplane of the adhesive for various preform adherend angles and for aluminum adherends and epoxy adhesive. Dimensions in centimeters (inches).**

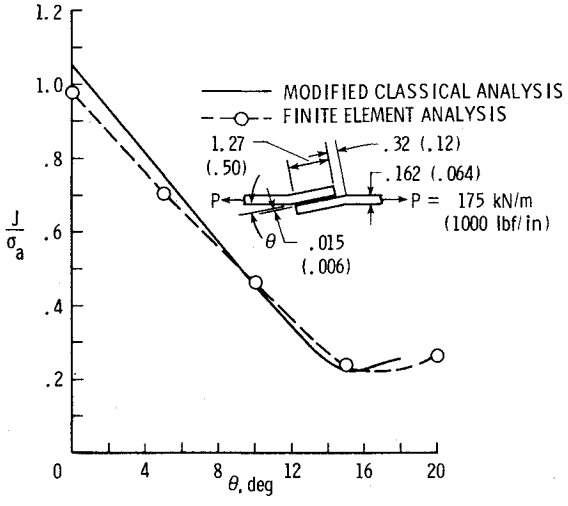


**Fig. 6 Effect of preform angle on the failure stress parameter for aluminum adherends and epoxy adhesive. Dimensions in centimeters (inches).**

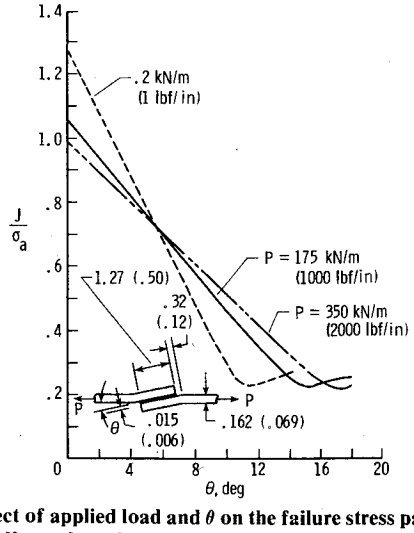


**Fig. 7 Effect of applied load and θ on the failure stress parameter for aluminum adherends and epoxy adhesive. Dimensions in centimeters (inches).**

parameter, then the lower the value of the computed stress parameter for a given load, the stronger the joint will be. Since the stress distribution is a nonlinear function of the applied load, it is appropriate to investigate the effect of variations of the adherend angle on the stress parameter for various load levels. For a lap joint with a 1.27-cm (0.5-in.)

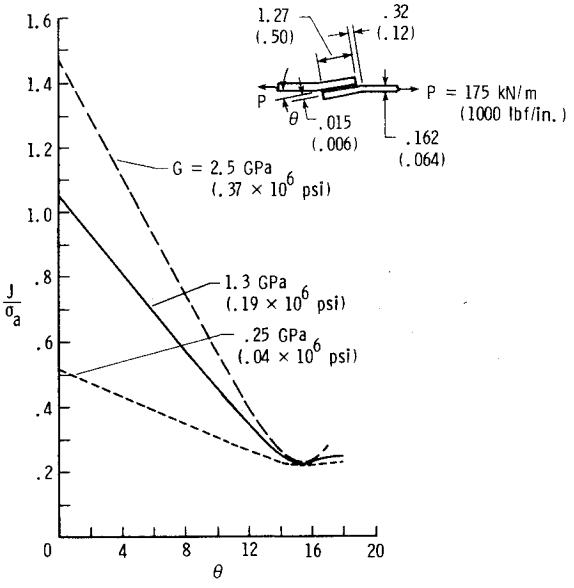


**Fig. 8 Effect of adhesive shear modulus and θ on the failure stress parameter for aluminum adherends. Dimensions in centimeters (inches).**

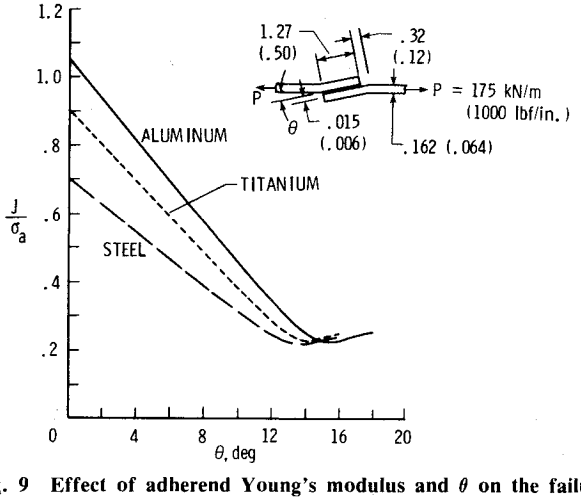


**Fig. 9 Effect of adherend Young's modulus and θ on the failure stress parameter for an epoxy adhesive. Dimensions in centimeters (inches).**

overlap, it can be seen from Fig. 7 that as the applied load is increased, the minimum stress parameter occurs at increasingly higher adherend preform angles. The optimum preform angle for a given application is dependent on the level of working stress of the adherend. However, the minimum value of the stress parameter is approximately the same for all load levels. For an adherend angle of approximately 5½ deg, the stress parameter seems to be independent of applied load.

The effects of adhesive shear modulus and adherend Young's modulus on the stress parameter are shown in Figs. 8 and 9, respectively. Decreasing the adhesive shear modulus (Fig. 8) and increasing the adherend Young's modulus (Fig. 9) result in lower values of the stress parameter for a given preform angle. However, the minimum stress parameter value and the preform angle at which it occurs are relatively insensitive to changes in adhesive shear modulus and adherend Young's modulus.

The effects of variations in the joint geometry are shown in Figs. 10-13. As seen from Fig. 10, the benefit from preforming the adherend is reduced as the adhesive thickness increases at the lower preform angles; however, the minimum stress parameter value and the preform angle at which it occurs is

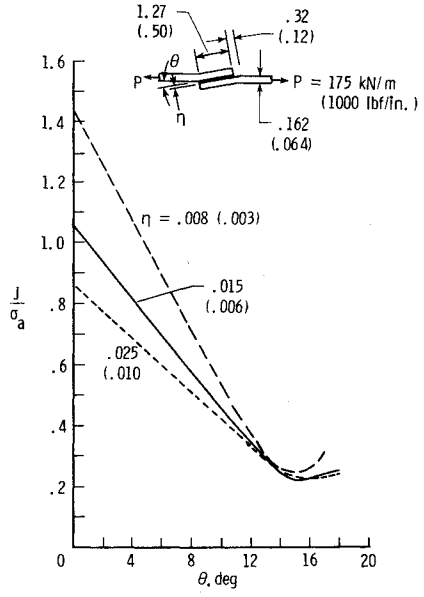


Fig. 10 Effect of adhesive thickness and $\theta$ on the failure stress parameter for aluminum adherends and epoxy adhesive. Dimensions in centimeters (inches).

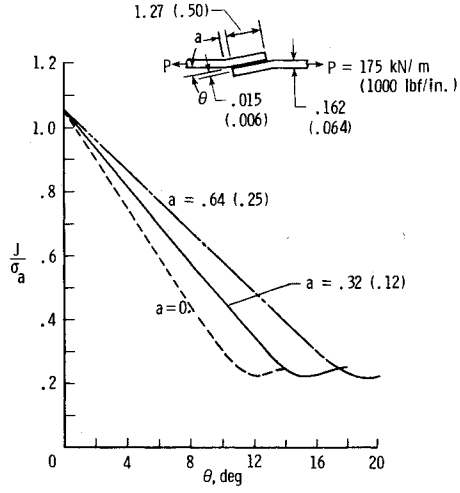


Fig. 11 Effect of "$a$" and $\theta$ on the failure stress parameter for aluminum adherends and epoxy adhesive. Dimensions in centimeters (inches).

not significantly affected by adhesive thickness for the range evaluated. Results shown in Fig. 11 indicate that the dimension "$a$," which is provided for ease of assembly of the joints, should be minimized to reduce the optimum adherend preform angle. From Fig. 12, as adherend overlap length increases, the optimum angle is reduced. As shown in Fig. 13, the optimum preform angle increases with increasing adherend thickness. Geometric variations of the adherend have a sizable effect on the preform angle at which the minimum value of the stress parameter occurs at a given applied load. The value of the minimum stress parameter, however, is nominally unaffected by this variation, except for some slight differences for adherend thickness.

For joints evaluated in this investigation with overlap lengths and adherend thicknesses sized so that bond strength is close to adherend strength, the optimum preform angle occurs between 12 and 18 deg. However, the results indicate that significant improvements in strength can be obtained at smaller preform angles. Therefore, the concept can be beneficially applied where other considerations restrict the size of the angle to a value smaller than that considered optimum.

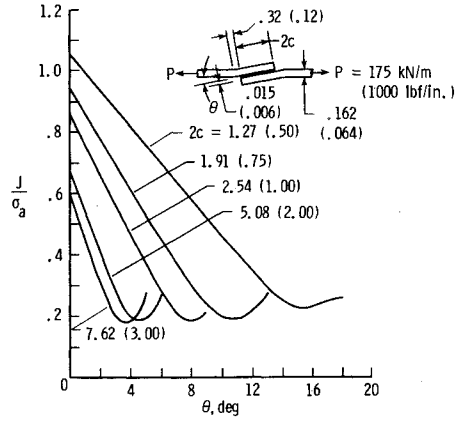


Fig. 12 Effect of overlap length and $\theta$ on the failure stress parameter for aluminum adherends and epoxy adhesive. Dimensions in centimeters (inches).

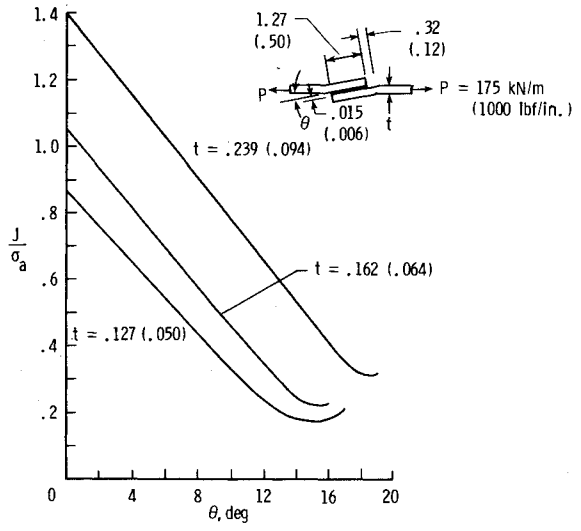


Fig. 13 Effect of adherend thickness and $\theta$ on the failure stress parameter for aluminum adherends and epoxy adhesive. Dimensions in centimeters (inches).

## Experiment

### Photoelastic Study

Two photoelastic lap joint models are examined to evaluate the effect of preforming the adherend on the stress distribution in the adherend. The adherends of the models are fabricated from a photoelastically sensitive epoxy material, PSM-5,‡ and are sized to approximate the geometric ratios of the ASTM D 1002-72 test specimen.[6] The lap joints have an epoxy material, PS-3,‡ bonded with PMC-1‡ adhesive between the adherends to represent an adhesive with a shear modulus one-fifteenth the shear modulus of the adherend. The modified classical analysis is used to compute the optimum preform angle for a lap joint with material properties and dimensions of the experimental model. The optimum angle is 18 deg. The stress field in the adherend in the region of the overlap is assumed to reflect the behavior in the adhesive. Photographs of the dark field isochromatic fringe patterns for the straight and preformed models subjected to the same load are shown in Fig. 14. The straight lap model has a maximum fringe order and, thus, maximum principal shear stress four times greater than the preformed adherend model at the edge of the overlap region near the bond line. The preformed adherend joint also has a more uniform principal shear stress distribution in the adherend than the straight lap joint has, as would be expected from the analysis.

‡Photolastic Company designation.

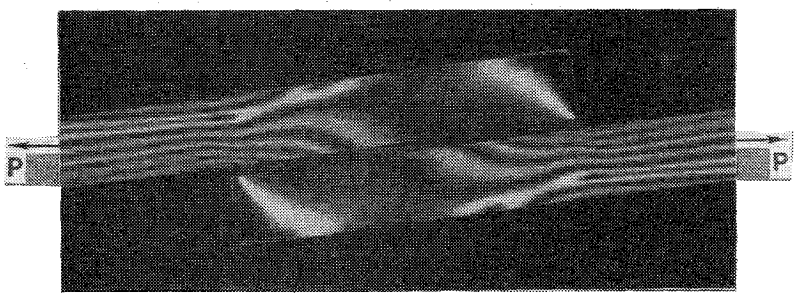


a)

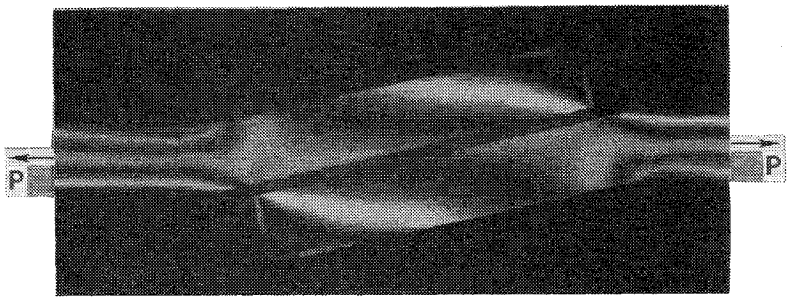


b)

**Fig. 14 Photoelastic fringe patterns for a) straight and b) preformed single lap joints, $P = 134$ N (30 lbf).**

**Table 2 Static and fatigue test specimens**

| Specimen description, cm (in.) | Preform angle $\theta$, deg | Static test specimens: No. of replicates | Static test specimens: Average failure load, kN/m (lbf/in.) | Fatigue test specimens: No. of replicates |
|---|---|---|---|---|
| $2c = 0.95$ (0.38) | 0 | 6 | 178 (1019) | — |
| $t = 0.162$ (0.064) | 5 | 6 | 171 (978) | — |
| $a = 0.32$ (0.12) | 10 | 6 | 173 (990) | — |
| $\eta = 0.010$ (0.004) | 15 | 6 | 169 (965) | — |
| | 20 | 6 | 133 (758) | — |
| $2c = 1.27$ (0.50) | 0 | 24 | 240 (1372) | 7 |
| $t = 0.162$ (0.064) | 5 | 24 | 269 (1536) | — |
| $a = 0.32$ (0.12) | 10 | 24 | 307 (1755) | 7 |
| $\eta = 0.010$ (0.004) | 15 | 24 | 302 (1726) | — |
| | 20 | 24 | 299 (1707) | — |
| $2c = 2.54$ (1.00) | 0 | 8 | 348 (1986) | — |
| $t = 0.476$ (0.188) | 5 | 3 | 460 (2625) | — |
| $a = 0.32$ (0.12) | 10 | 4 | 542 (3096) | — |
| $\eta = 0.010$ (0.004) | 15 | 4 | 573 (3841) | — |
| | 20 | 4 | 649 (3706) | — |
| $2c = 4.44$ (1.75) | 0 | 4 | 572 (3265) | 10 |
| $t = 0.64$ (0.25) | 5 | 4 | [a] | — |
| $a = 0.64$ (0.25) | 10 | 4 | [a] | — |
| $\eta = 0.010$ (0.004) | 15 | 4 | 1261 (7200) | 13 |
| | 20 | 4 | 1232 (7035) | — |

[a] Improperly bonded.

### Metallic Joint Tests

*Specimens and Tests*

Approximately 230 bonded preformed single lap joint test specimens with dimensions given in Fig. 1 and Table 2 are tested in this investigation. Specimens with preform angles of 0, 5, 10, 15, and 20 deg are tested. The adherends are made of 2024-T3 aluminum and are bonded using EA 934§ epoxy adhesive. The specimens are made in groups of four using two sets of four-finger specimen blanks as suggested in Ref. 5. The adherends are bent to the correct angle, bonded and cured as prescribed by the adhesive manufacturer, and cut into individual test specimens. The adhesive bond thickness is controlled using glass beads and checked by measuring the total joint thickness at three places across the center of the joint and then subtracting the adherend thickness. The specimens are mounted in the test machine using wedge action tension grips with universal joints above and below the grips for load alignment. The free distance between the grips was maintained at 12.7 cm (5.0 in.) plus the overlap length for each test.

For the static tests, the lap joint specimens are loaded to failure in tension. The tests are conducted at a constant displacement rate of 0.13 cm/min (0.05 in./min).

§Hysol Division, Dexter Corporation designation.

The fatigue tests are conducted by sinusoidal cycling of the load between 10% of the average static tensile ultimate strength of the joint and the maximum cyclic tensile test load. The machine is operated in a load control mode at a rate of 1800 cycles/min. The loading history waveform is monitored using an oscilloscope.

*Static Test Results*

A plot is given in Fig. 15 of the effect of preform angle on the average static tensile failure load of test specimens (see Table 2) with overlap lengths ranging from 0.95 to 4.44 cm (0.375 to 1.75 in.). The failure load shown for each overlap length is normalized by the average failure load (given in Table 2) for the straight lap joint with the same overlap length. Preforming the adherends increases the average static ultimate load for three of the four configurations tested. The increases range from about 30% for overlap lengths of 1.27 cm (0.50 in.) to 120% for overlap lengths of 4.44 cm (1.75 in.). Maximum loads occur for preform angles between 10 and 15 deg, as suggested by the failure stress parameter; however, the increase in failure load expected from examination of the failure stress parameter is not obtained. The dramatic increase in load-carrying capacity for the larger overlap lengths shown in Fig. 15 indicates that a design concept using preform adherends may extend the load range for which bonded single lap joints can be used.

*Fatigue Test Results*

Fatigue data are shown in Fig. 16 for two sets of straight lap joints with overlap lengths of 1.27 and 4.44 cm (0.5 and 1.75 in.) and preformed joints with the same overlaps. The data points shown for the single cycle failure (static strength) are the average of replicate tests. Each multicycle failure test point represents a single test. For specimens with the smaller overlap length, the number of cycles to failure can be increased two orders of magnitude for a given stress by preforming the adherends 10 deg. The specimens with the larger overlap can withstand loads almost 100% greater than corresponding straight lap joints up to $10^5$ cycles by preforming the adherends 15 deg. Thus, sizable benefits can be obtained in the low-cycle fatigue life or in additional load capacity of bonded single lap joints by preforming the adherends.

**Discussion of Adhesive Shear Strength Methods**

Tensile tests of bonded single lap joints with straight adherends are the most common tests used to evaluate the ultimate shear strength of adhesives (see ASTM D 1002-72, Ref. 5). Because single lap joints have high stress concentrations near the edge of the overlap region for both shear and peel, the test results can be misleading. For example, lap joints which fail because of low peel strength in the adhesive could lead one to conclude that the adhesive shear strength was low. Several alternative test procedures which give a closer approximation to the ultimate shear strength of adhesive have been proposed including napkin ring[7] tests and thick adherend[8] tests. These tests, however, are either 1) difficult to control; 2) costly, especially when used to obtain allowable values; or 3) cannot be easily modified for use with orthotropic adherends such as fiber-reinforced composite materials. A comparison of the average ultimate shear values obtained using the ASTM D 1002-72 test specimen, the same test specimen with preformed adherends, and the thick adherend test specimen can be made using results shown in Table 3. The thick adherend data are an average of ten tests conducted using EA 934 epoxy adhesive and aluminum adherends with dimensions similar to those given in Ref. 8. For the most commonly used overlap length of 1.27 cm (0.50 in.), the ASTM D 1002-72 specimen, gives ultimate shear

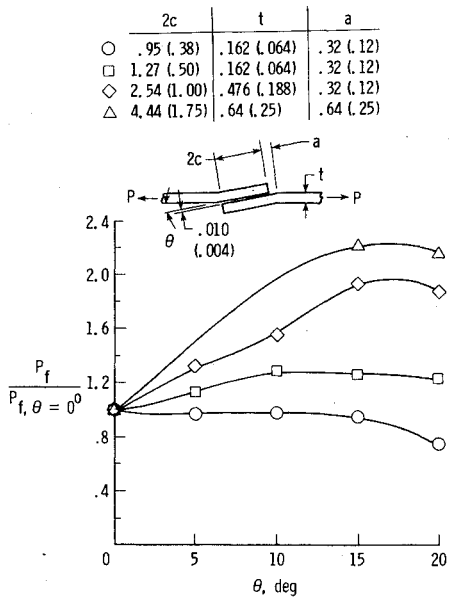


**Fig. 15 Effect of preform angle on tensile failure load for various overlap lengths. Dimensions in centimeters (inches).**

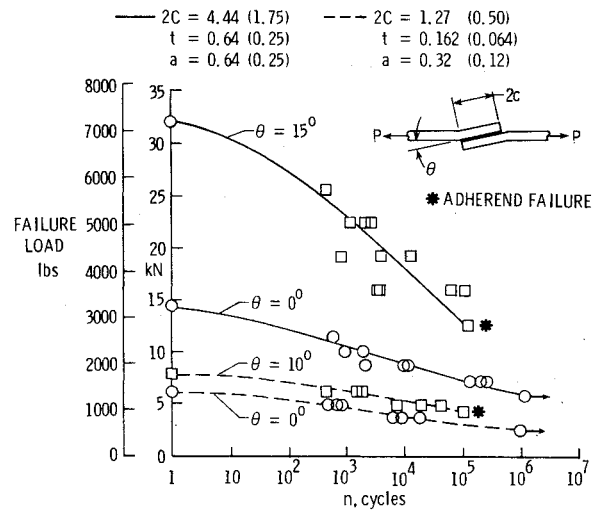


**Fig. 16 Effect of preform angle on fatigue strength for various overlap lengths. Dimensions in centimeters (inches).**

**Table 3 Ultimate shear strength values from tests of different type specimen**

| Specimen (aluminum adherends and EA 934 epoxy adhesive) | Adherend thickness, cm (in.) | Average shear stress, MPa (psi) $2c =$ 1.27 cm (0.50 in.) | $2c =$ 2.54 cm (1.00 in.) | $2c =$ 4.44 cm (1.75 in.) |
|---|---|---|---|---|
| ASTM D-1002-72 | 0.162 (0.064) | 18.6 (2700) | 13.7 (1990) | 12.9 (1870) |
| ASTM D-1002-72 with preform adherend | 0.162 (0.064) | 24.1 (3500) | 26.5 (3840) | 28.4 (4110) |
| Thick adherend | 1.27 (0.50) | 34.5 (5000) | — | — |

values approximately 54% of those given by the thick adherend tests, whereas the preformed specimen gives a value approximately 70% of that obtained from the thick adherend tests. For an increase in overlap length, the indicated ultimate shear values obtained using the ASTM D 1002-72 test specimen decrease. For the test with preformed adherends, an increase in the overlap length results in a shear ultimate value which approaches that given by the thick adherend tests. Because the specimens with preformed adherends are relatively inexpensive and can be used with orthotropic adherends, the results indicate that they might offer an attractive alternative to both the ASTM D 1002-72 tests and the thick adherend tests.

## Concluding Remarks

A theoretical and experimental investigation is conducted on bonded single lap joints with preformed adherends. The adherends are preformed before bonding to reduce the angle between the line of action of the applied in-plane force and the bond line. Results from the analysis indicate that preforming the adherends reduces the moment resultant in the adherend at the edge of the overlap region which causes a reduction in both the peel and shear stresses and gives a more uniform shear distribution in the adhesive. Preforming the adherends up to 15 deg causes at least a threefold reduction in the maximum shear and peel stress in the midplane of the adhesive. A parametric study is conducted to determine the optimum preform angle for typical adherend and adhesive material properties and joint geometries. The optimum preform angle for joints with overlap length and adherend thickness sized so that bond strength is close to adherend strength occurs between 12 and 18 deg.

Increases in static load transfer of up to 120% are shown experimentally, and several orders-of-magnitude increase in fatigue life have been achieved. Thus, by preforming the adherends, sizable benefits can be obtained in the fatigue life or additional load capacity of bonded single lap joints.

## Appendix—Modified Classical Analysis Solution

The development of the shear and peel stress equations is similar to that of Refs. 2 and 3, but a consistent assumption of plate behavior is assumed throughout the development; whereas in the above references, beam theory is used for load-displacement equations and boundary conditions while plate theory is used to develop the moment equilibrium equations. The sign convention and geometric symbols used in the analysis are shown in Fig. A1. The equations for the adhesive shear and peel stresses are

$$\tau=\frac{P\cos\phi}{cS}\left\{\left[\frac{D}{A}+\left(\frac{t}{2}\right)^2 k\right]\frac{\delta}{\sinh\delta}\cosh\frac{\delta x_3}{c}+\frac{t}{2}\left[\left(\frac{t+\eta}{2}\right)-\frac{t}{2}k\right]\right\}$$

and

$$\sigma=\frac{Pt\cos\phi}{c^2\Delta}\left\{\left[\lambda^2\frac{k}{2}r_1+\lambda k'\sinh\lambda\sin\lambda\right]\sinh\frac{\lambda x_3}{c}\sin\frac{\lambda x_3}{c}+\left[\lambda^2\frac{k}{2}r_2+\lambda k'\cosh\lambda\cos\lambda\right]\cosh\frac{\lambda x_3}{c}\cos\frac{\lambda x_3}{c}\right\}$$

where

$$\cos\phi=\frac{\ell+c}{e},\qquad e=\sqrt{b^2+(\ell+c)^2}$$

$$b=(\ell-a)\tan\theta+\frac{t+\eta}{2},\qquad S=\frac{2D}{A}+t\left(\frac{t+\eta}{2}\right)$$

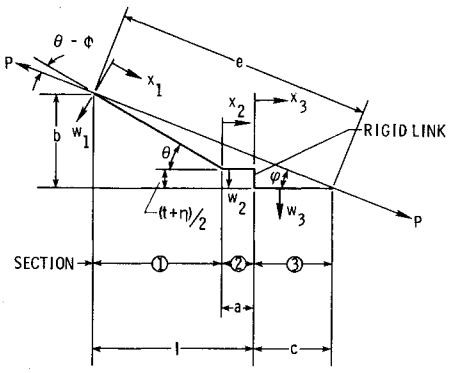


**Fig. A1 Nomenclature and sign convention used in modified classical analysis.**

$$k=-\frac{2}{t}\left[w_2(a)+(\ell-a)\tan\theta-\ell\tan\phi\right]$$

$$\tan\phi=\frac{(\ell-a)\tan\theta+\left(\frac{t+\eta}{2}\right)}{\ell+c},\qquad \delta=c\sqrt{\frac{G_a S}{\eta D}}$$

$$\Delta=\tfrac{1}{2}(\sin 2\lambda+\sinh 2\lambda),\qquad \lambda=c\sqrt[4]{E_a/2\eta D}$$

$$k'=\frac{c}{t}\left[\tan\phi-\frac{dw_2(a)}{dx_2}\right],\qquad r_1=\cosh\lambda\sin\lambda+\sinh\lambda\cos\lambda$$

$$r_2=\sinh\lambda\cos\lambda-\cosh\lambda\sin\lambda$$

where for isotropic adherends of modulus $E$ and Poisson's ratio $\nu$,

$$D=\frac{Et^3}{12(1-\nu^2)}\qquad\text{and}\qquad A=\frac{Et}{1-\nu^2}$$

The displacement in the overlap region, $w_2$, is found by the simultaneous solution of the equations of equilibrium for each of the three sections of the lap joint as shown in Fig. A1. Each section is assumed to deform as a wide beam subject to the governing equation

$$\frac{d^2 w_i}{dx_i^2}=-\frac{M_i}{D_i}\qquad\text{for regions}=1,2,3$$

where $M_i$ is the cross-sectional moment and $D_i$ is the flexural stiffness of the $i$th section.

The six boundary and continuity conditions are:

$$w_1(0)=0,\qquad w_3(c)=0$$

$$w_1\left(\frac{\ell-a}{\cos\alpha}\right)=w_2(0)\cos\theta,\qquad w_2(a)=w_3(0)$$

$$\frac{dw_1\left(\frac{\ell-a}{\cos\theta}\right)}{dx_1}=\frac{dw_2(0)}{dx_2},\qquad \frac{dw_2(a)}{dx_2}=\frac{dw_2(0)}{dx_3}$$

The displacement solution for section 2 is given by

$$w_2(x)=C_2\sinh\beta_2 x_2+F_2\cosh\beta_2 x_2+(x_2-c-a)\tan\phi+\frac{t+\eta}{2}$$

where

$$\beta_2 = \sqrt{P\cos\phi / D_2}$$

The considerable algebraic manipulation required to find the solution constants $C_2$ and $F_2$ is performed using the symbolic manipulation computer code MACSYMA,[9] and the resulting expressions are too long to include here.

## References

[1] Mylonas, C., "On the Stress Distribution in Glued Joints," *Proceedings of the 7th International Congress for Applied Mechanics,* 1948, pp. 137-149.

[2] Das Gupta, S. and Sharma, S. P., "Stresses in an Adhesive Lap Joint," ASME Paper 75-WA/DE-18, July 1975.

[3] Goland, M. and Reissner, E., "The Stresses in Cemented Joints," *Journal of Applied Mechanics,* pp. A-17-A-27.

[4] Cooper, P. A. and Sawyer, J. W., "A Critical Examination of Stresses in an Elastic Single Lap Joint," NASA TP-1507, Sept. 1979.

[5] "Standard Test Method for Strength Properties of Adhesives in Shear by Tension Loading (Metal-to-Metal)," ASTM D 1002-72, Pt. 22 of *1978 Annual Book of ASTM Standards,* c. 1978, pp. 253-257.

[6] Whetstone, W. D., "SPAR Structural Analysis System Reference Manual - System Level 13A, Vol. I: Program Execution," NASA CR-158970.

[7] Gillespe, T. and Rideal, Sir Eric, "The Deformation and Strength of Napkin Ring Metal-Adhesive-Metal Joints," *Journal of Colloid Science,* Vol. 11, May 1956, pp. 732-747.

[8] Renton, W. J. and Vinson, J. R., "Shear Property Measurements of Adhesives in Composite Material Bonded Joints," *Composite Reliability,* ASTM STP 580, 1975, pp. 119-132.

[9] *MACSYMA Reference Manual,* The Mathlab Group, Laboratory for Computer Science, M.I.T., Dec. 1977.